Clays Clay Miner., Vol. 70, No. 6:824–836, 2022
https://doi.org/10.1007/s42860-023-00219-7

ORIGINAL PAPER

Molecular Modeling to Predict the Optimal Mineralogy of Smectites as Binders of Aflatoxin

Marek Szczerba · Youjun Deng · Mariola Kowalik-Hyla

Accepted: 4 January 2023 / Published online: 2 February 2023

Abstract Numerous experiments have verified that smectites can adsorb aflatoxin B_1 (AfB_1) effectively and the efficiency of this process depends heavily on the chemical, physical, and mineralogical characteristics of the smectite. Several relationships between these characteristics and AfB_1 sorption have been determined experimentally, but the molecular mechanisms underlying these were not investigated. In the current study the effects of charge density, type of exchange cation, and charge origin (octahedral vs. tetrahedral) on AfB_1 sorption on smectites were analyzed by a series of molecular simulations. The calculations confirmed the formation of water bridges between carbonyl groups of AfB_1 molecules and interlayer cations. Flat orientation of AfB_1 molecules on smectite surfaces was also confirmed. For larger amounts of AfB_1 molecules in the intercalates, self-association of two AfB_1 molecules bound by π–π interaction was shown. The thermodynamics of AfB_1 sorption depends heavily on the water content in the structure, being optimal for basal distances corresponding to two layers of water. A clear preference for sorption of AfB_1 on smectites with bivalent cations (Ba^{2+}, Ca^{2+}) and an octahedral origin of its layer charge was confirmed and this was explained as steric hindrance between hydrated ions and AfB_1 molecules, which tend to lie flat on smectite surfaces devoid of ions. Ba-montmorillonite with a charge of 0.4 per half unit cell was shown to have the smallest and thus the best potential energy of adsorption compared to the other layer charges.

Keywords Adsorption · Aflatoxin B1 · Molecular simulations · Smectite

Associate Editor: Eric Ferrage

Supplementary Information The online version contains supplementary material available at https://doi.org/10.1007/s42860-023-00219-7.

M. Szczerba (✉) · M. Kowalik-Hyla
Institute of Geological Sciences, Polish Academy of Sciences, Kraków 31002, Poland
e-mail: m.szczerba@ingpan.krakow.pl

Y. Deng
Department of Soil and Crop Sciences, Texas A&M University, College Station, TX 77843-2474, USA

Introduction

The occurrence of aflatoxins (Aflatoxin B_1, or AfB_1, is the most common example), a group of carcinogenic mycotoxins, in agricultural products appears to be unavoidable due to heat, drought, humidity, insect stresses, or combinations of these factors. Deactivation of the toxins in food and feed, and removal of the toxins during biofuel production as the last defensive measures are needed to prevent the harmful effects of aflatoxins on humans and animals. Many chemical, physical, and biological detoxification methods have been proposed but are used rarely in practice due to

cost, side effects, or cultural acceptance barriers. One economically feasible and environmentally safe solution for aflatoxin detoxification is to use clays, especially bentonites, as aflatoxin binders (e.g. Magnoli et al., 2008; Masimango et al., 1979; Phillips et al., 1988).

Over the last four decades, many adsorption experiments and animal and clinical trials have proved that bentonite clays can adsorb aflatoxins and can reduce the toxicity of aflatoxins to animals and humans (Awuor et al., 2017; Colvin et al., 1989; Kubena et al., 1990; Maki et al., 2016; Mitchell et al., 2014; Pollock et al., 2016). As smectites are the dominant clay mineral in bentonites, efforts have been made to reveal the most important mineralogical, physical, and chemical properties that determine the efficiency of smectites in aflatoxin detoxification (e.g. Barrientos-Velazquez et al., 2016a; Deng et al., 2012; Deng & Szczerba, 2011). Studies have revealed a >10-fold difference in aflatoxin adsorption capacity among bentonites (Kannewischer et al., 2006), and that the layer charge density, type of exchange cation, and origin of the layer charge source had determinative roles in aflatoxin binding efficiency (Barrientos-Velazquez et al., 2016b; Deng et al., 2012), whereas the type of octahedral sheets (dioctahedral vs. trioctahedral) showed little difference in their binding capacity (Barrientos-Velazquez et al., 2016b). Many efforts have been made to increase the binding capacity and selectivity of smectites in gastric fluids by heating, replacing the exchange cation, and pillaring with inorganic polycations or organic molecules (Barrientos-Velazquez & Deng, 2020; Jaynes et al., 2007; Khan et al., 2022; Wang et al., 2017).

These experimental observations yield critical information about the mineralogical properties needed for aflatoxin binding. Retrieval from the experimental data of the optimal structural information about the binders is difficult due to limitations on specimen availability to cover the ranges of structural parameters for the test. To find optimal parameters that determine the adsorption selectivity and capacity of the smectites for aflatoxins, molecular modeling may be useful.

Preliminary molecular dynamics (MD) simulations on aflatoxin–smectite interactions demonstrated that molecular modeling was very useful in verifying and fine-tuning aflatoxin–smectite interaction mechanisms at the atomic level (Deng & Szczerba, 2011), but only limited scenarios were simulated in that study. The objective of the current study was to simulate more systematically the influence of smectite charge density, exchange cation type, smectite charge origin, and water content on the adsorption of aflatoxin B_1.

Methodology

Molecular Simulations

The following five factors were varied during the molecular dynamics simulation: charge origin (octahedral vs. tetrahedral), charge density, type of exchange cation, water content, and AfB_1 loading level. The ranges of variation for each of these factors were as follows:

(1) Charge origin and layer charge density: six dioctahedral smectites were simulated in this study; three montmorillonites (Mnt) with octahedral-sheet charge densities of 0.3, 0.4, and 0.5 charge per half unit cell (cphuc) and three beidellites (Bei) with tetrahedral-sheet charge densities of 0.3, 0.4, and 0.5 cphuc. The exact chemical formulae of the 2:1 layers studied were $(Al_{1.7}Mg_{0.3})Si_4O_{10}(OH)_2$, $(Al_{1.6}Mg_{0.4})Si_4O_{10}(OH)_2$, $(Al_{1.5}Mg_{0.5})Si_4O_{10}(OH)_2$, $Al_2(Si_{3.7}Al_{0.3})O_{10}(OH)_2$, $Al_2(Si_{3.6}Al_{0.4})O_{10}(OH)_2$, and $Al_2(Si_{3.5}Al_{0.5})O_{10}(OH)_2$ for Mnt03, Mnt04, Mnt05, Bei03, Bei04, and Bei05, respectively.

(2) Type of exchange cations: Deng et al. (2012) showed that divalent cation saturation of smectites led to greater aflatoxin adsorption than monovalent cation saturation, and Ba^{2+} saturation yielded the greatest AfB_1 adsorption capacity. Ba^{2+} saturation was used in most of the simulations, therefore.

(3) To verify the effect of exchange cation, simulated montmorillonites of charge density 0.4 cphuc with Ca^{2+} and Na^{+} saturations were included in the simulation.

(4) Six levels of water contents in the smectites (0, 3.75, 7.5, 11.25, 15, and 18.75 mol/kg), and

(5) Six levels of the amount of AfB_1 adsorbed (0, 0.185, 0.37, 0.555, 0.74, and 0.925 mol/kg) were used in the simulations.

https://doi.org/10.1007/s42860-023-00219-7 Published online by Cambridge University Press

In total, eight smectite models were taken into account and they were coded by the mineral species (Mnt and Bei), layer charge density (e.g. 03 for 0.3 cphuc), and the type of exchange cation: Mnt03_Ba, Mnt04_Ba, Mnt04_Ca, Mnt04_Na, Mnt05_Ba, Bei03_Ba, Bei04_Ba, and Bei05_Ba. For each of the eight smectite models, the combinations of water and AfB_1 contents resulted in 36 simulations. A total of 288 molecular dynamics simulations were conducted for the various AfB_1-smectite complexes.

In the simulations, the SPC force field was assumed for water molecules (Berendsen et al., 1981), *CLAYFF* for smectites (Cygan et al., 2004), and *GAFF* for AfB_1 molecules (general AMBER force field; Wang et al., 2004). For each smectite model, a supercell was built as 8×4×2 unit cells in the *a*, *b*, and *c* crystallographic directions. The simulated aflatoxin-smectite system had a size of ~41.6 Å×36.1 Å×*X* Å, with the value of *X* dependent on the amounts of AfB_1 and water in the interlayer spaces.

For these initial structures, energy minimizations were performed first, followed by NPT-ensemble MD simulations at 1 atm, in temperature cycles. During the first period of every temperature cycle, the temperature was set at 378 K and the simulation was run for 150 ps. Then the temperature was reduced to 298 K, and simulation continued for 300 ps. This MD simulation cycle was repeated three times in order to optimize distribution of molecules in the interlayer. The last period of simulation at 298 K was run for 600 ps from which the system properties were recorded for further analysis from the last 300 ps. The Langevin dynamics protocol was used to control the temperature and Langevin piston to control the pressure. The timestep was set at 1 fs and the dynamic trajectories and system properties were recorded every 1 ps. During the NPT simulations the relaxation of the simulation cell was performed in all *a*, *b*, and *c* crystallographic directions and the clay structure was allowed to be flexible and free to move in all directions to optimize positions of layers in the *a*-*b* plane. All the simulations were performed using the *LAMMPS* computer program (Plimpton, 1995).

Analysis of the MD Simulation Results

For each hydration level, the energy of the aflatoxin molecule adsorption on smectite was calculated from the following equation (1):

$$\Delta U(N)_{AfB_1} = \frac{< U(N) > - < U(0) >}{N} \quad (1)$$

where: $\langle U(N) \rangle$was the average potential energy of an equilibrium system with *N* aflatoxin molecules and a certain number of water molecules in the interlayer, and $\langle U(0) \rangle$ was the average potential energy of an equilibrated system containing only a certain number of water molecules, used as a reference state.

A similar equation was used for calculation of hydration of aflatoxin-clay complexes with the same AfB_1 content but a variable number of water molecules: $\Delta U(N)_{H2O}$.

In addition, the energy of aflatoxin addition to various smectites was calculated taking the following reaction into account:

$$\text{smectite/water} \overset{+AfB1}{\rightarrow} \text{smectite/water/AfB}_1 \quad (2)$$

including all contributions (molecular, van der Waals, and electrostatic) to total potential energy. A specified amount of water and AfB_1 was considered in the complex on the right side: 0.37 mol/kg of AfB_1 and 7.5 mol/kg water.

For comparison, the energy of a single AfB_1 molecule addition to water was also calculated:

$$\text{water} \overset{+AfB1}{\rightarrow} \text{water/AfB}_1 \quad (3)$$

This energy was generated by a separate calculation for a water box consisting of 500 molecules (NPT ensemble, 2 ns simulation).

Results and Discussion

Dependence of Basal Spacing on the Amount of Aflatoxin and Water in the Complex

In the ranges of water and aflatoxin contents simulated, the basal spacing of the smectite varied from 9.8 to 27 Å. Increasing the water or AfB_1 contents generally led to an increase in basal d_{001} spacing (Fig. 1). No significant difference was noted in terms of interlayer expansion for structures with small water contents (0 and 3.7 mol/kg H_2O). This was due to the existence of empty void spaces between aflatoxin molecules in dry structures, which could be then filled with H_2O. For larger amounts of AfB_1 and H_2O, the

https://doi.org/10.1007/s42860-023-00219-7 Published online by Cambridge University Press

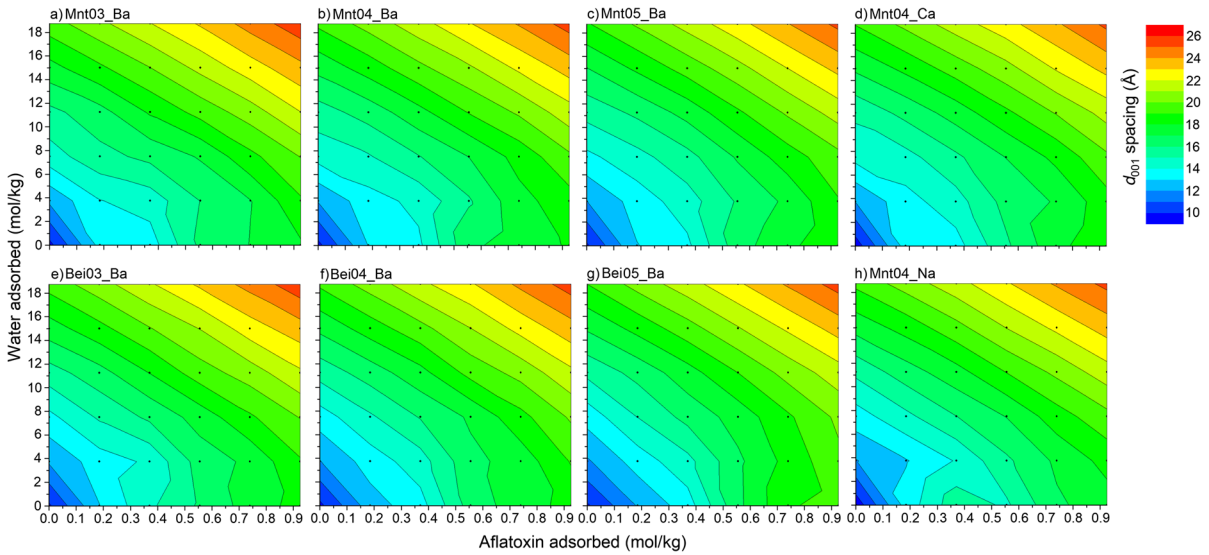

Fig. 1 Dependence of d_{001} spacing of AfB_1-smectite complexes on AfB_1 and water content. The contour graphs were based on the 36 data points of molecular simulations

basal spacing increased linearly with the contents of both molecules. For these smectite structures, water molecules filled the space between AfB_1 molecules, and the addition of new molecules led to expansion of interlayer distances.

In the literature, the greatest d_{001} spacing of air-dried AfB_1-smectite complexes recorded at room temperature and ~60% humidity was ~15 Å (e.g. Deng et al., 2010). Basal spacings of >20 Å observed in high-water content conditions in these simulations offered more insight into to the AfB_1-smectite interactions in solution. As most X-ray diffraction analyses of AfB_1-smectite complexes were analyzed after drying the complexes, the *d* spacings of >20 Å in the presence of large amounts of water deserve experimental verification. Even at 0 mol/kg of water, the basal spacing of the AfB_1-smectite could be expanded to >18 Å when AfB_1 adsorption reached 0.9 mol/kg. Neither a large basal spacing like this nor this level of adsorption has been observed experimentally.

Influence of the Water Content on the Configurations of Adsorbed Aflatoxin in the Interlayer of Smectite

Water content affected to a great extent the orientations and configurations of the aflatoxin molecules adsorbed in the interlayer of the smectites. The individual aflatoxin molecules did not deform significantly from their nearly planar structure when the water content was varied, but the distribution of the AfB_1 molecules varied drastically when the interlayer water content was increased. For example, at the 0.37 mol/kg AfB_1 adsorption level, when the complexes were dry, the adsorbed AfB_1 molecules were oriented nearly parallel to the basal surfaces of the smectites with only one layer of the AfB_1 molecules scattered uniformly in the interlayer space (Fig. 2a). When the amount of water was increased to 7.5 mol/kg, AfB_1 molecules formed two layers (Fig. 2b). For a water content of 18.75 mol/kg, the AfB_1 molecules had more random orientations, and some of the aflatoxin molecules had inclination angles toward the basal surfaces of >60° (Fig. 2c). Introducing water into the AfB_1-smectite complexes made both the exchange ions and aflatoxin molecules more mobile and more dispersed in the interlayer. For larger AfB_1 loadings, some of AfB_1 molecules can be disoriented from parallel orientation, also for structures without water (Supplementary Materials, Fig. S1a). Addition of water molecules led to more random orientations of AfB_1 molecules for these structures (Fig. S1b, 1c), similarly as in the case of smaller AfB_1 loadings.

Aflatoxin molecules moved around in the interlayer and started stacking on each other at large water contents. They formed two-layer or even three-layer structures in some locations. A unique feature of

https://doi.org/10.1007/s42860-023-00219-7 Published online by Cambridge University Press

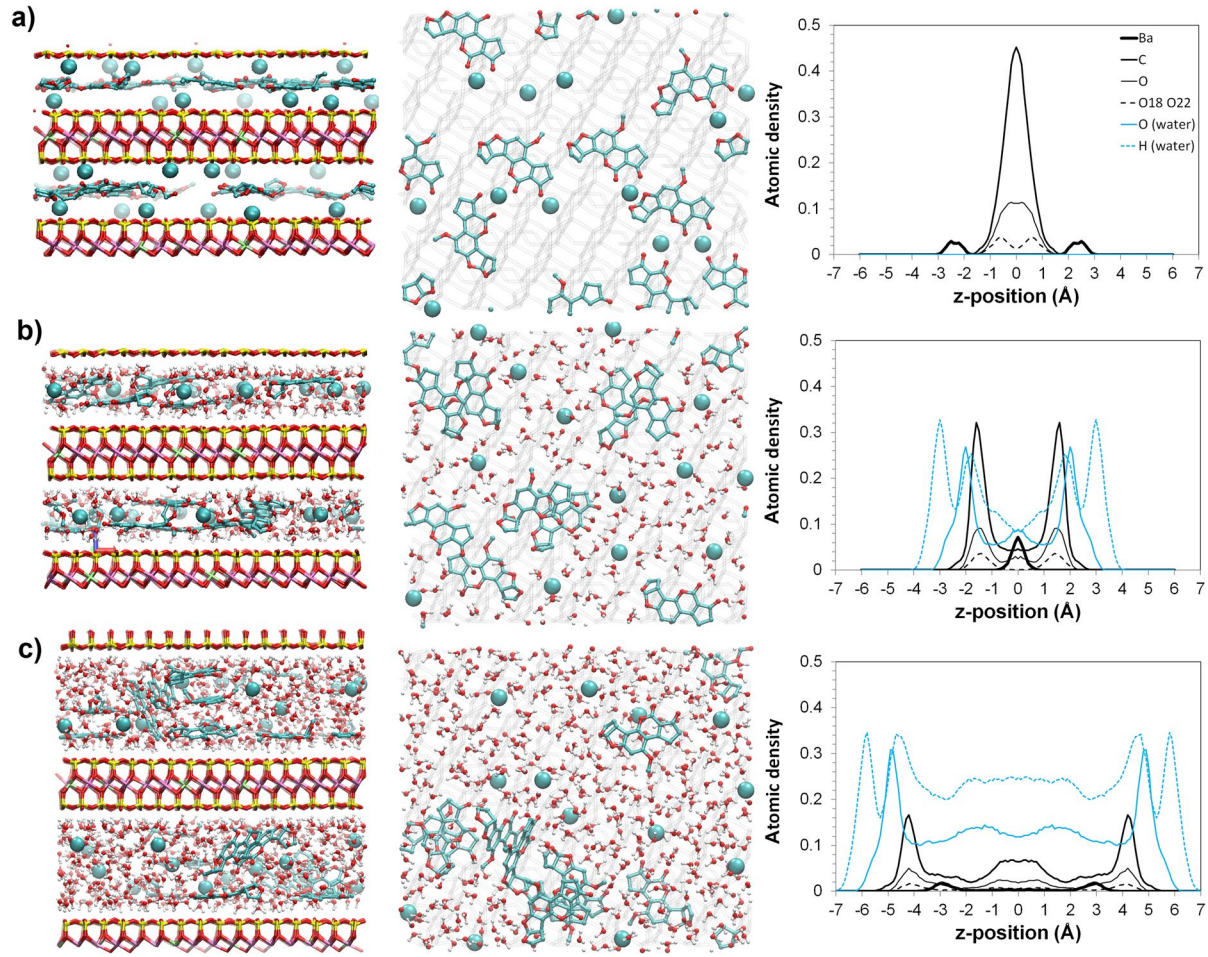

Fig. 2 Structure of Mnt04_Ba smectite with 0.37 mol/kg aflatoxin B_1 adsorbed: **a** dry; **b** with 7.5 mol/kg water; **c** with 18.75 mol/kg water adsorbed. Side view, top view, and distribution of atoms are shown in consecutive columns from left to right. The formation of AfB_1 π–π complexes for structures with water is visible

self-association of aflatoxin molecules was observed on the structure corresponding to a larger amount of adsorbed water (Fig. 2b, c). In this self-associated AfB_1 structure, the aflatoxin molecules could form π–π stacking complexes, and the self-associated AfB_1 molecules excluded water to their surrounding spaces. With increasing numbers of water molecules, these π–π complexes could detach from the surface and disperse in the interlayer water (Fig. 2c). The self-association of AfB_1 molecules in the interlayer of smectite appeared to be consistent with the low water solubility of the toxin of 20–30 mg/L. Such a feature would be difficult to detect experimentally with spectroscopic methods.

The simulations also showed that, as expected from the experimental IR data of Deng et al. (2010, 2012), mainly water bridges were formed between ions and aflatoxin carbonyl oxygen atoms as indicated by the radial distribution function (RDF) and running coordination number (RCN) plots between interlayer Ba^{2+} cations and carbonyl oxygens (Fig. 3). The first peak at ~2.8 Å on the RDF patterns was due to the direct Ba-carbonyl ion–dipole interactions and the second peak at radius of ~4.8–5.3 Å was due to the formation of water bridges between the exchange cation and the carbonyl groups. The peaks on the RDF patterns corresponded to the growth of the RCN function. The simulated ratio between the amount of water-bridged Ba to directly coordinated

https://doi.org/10.1007/s42860-023-00219-7 Published online by Cambridge University Press

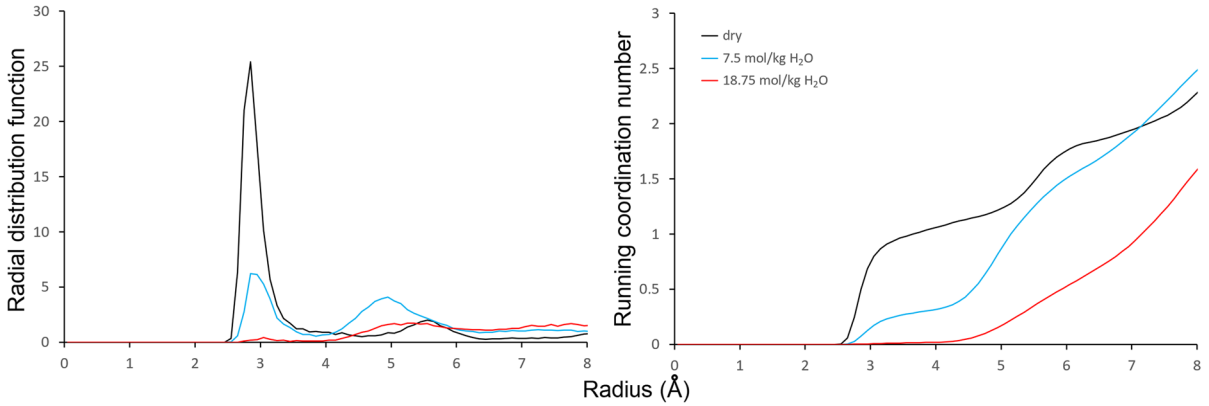

Fig. 3 Radial distribution function and running coordination number plots for Ba–$O_{carbonyl}$ of AfB_1 for the Mnt04_Ba structure with 0.37 mol/kg of AfB_1 and variable amounts of water adsorbed

Ba was ~5.5:1 at the 7.5 mol/kg water content, and 40:1 for a water content of 18.75 mol/kg (calculated based on data from Fig. 3). These calculations suggested the importance of water bridging for the adsorption of AfB_1 by the wet smectites, but the simulation also suggested the direct ion–dipole interaction still made significant contributions to the bonding. The exchange cations can have the ion–dipole interactions with the oxygen atoms on the dihydrofuran rings (Fig. 2).

The calculated energies of aflatoxin molecule adsorption (Eq. 1) of the AfB_1-smectite complexes showed minima at water content levels of 7.5 mol/kg for all five montmorillonite structures that had layer charge which originated from the octahedral sheet (Fig. 4a, b, c, d, h). This amount corresponded to two layers of water in the interlayer of the smectites and gave a basal spacing of close to 15 Å. This basal spacing was in agreement with the experimental observation that the synthesized AfB_1-smectite had a basal spacing of ~15 Å at room humidity (Deng et al., 2010). With either more or less water, energies of AfB_1 molecule adsorption increased.

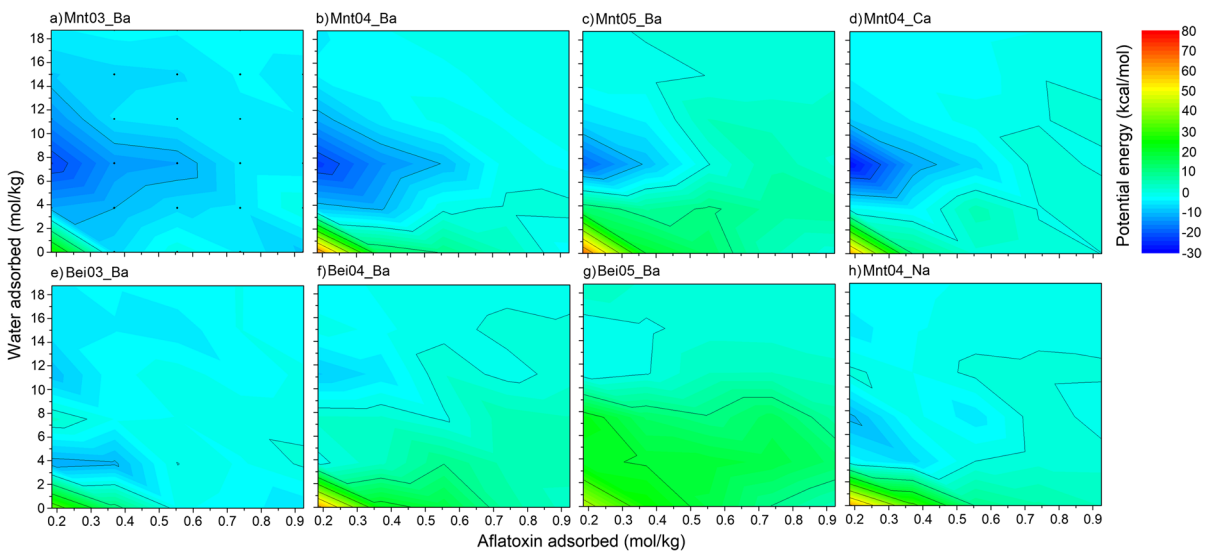

Fig. 4 Potential energies (kcal/mol) of adsorption of aflatoxin molecules on smectite structures. Smectite at a certain hydration level but without AfB_1 molecules was used as a reference state; note, therefore, that the amount of AfB_1 sorbed begins at 0.185 mol/kg

https://doi.org/10.1007/s42860-023-00219-7 Published online by Cambridge University Press

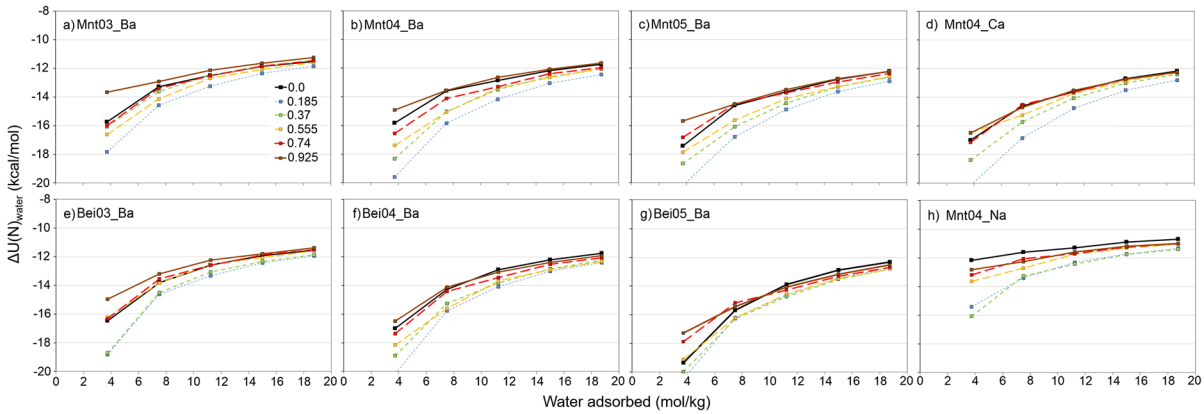

Fig. 5 Potential energies (kcal/mol) of water-molecule adsorption on smectite structures. Smectite with a certain number of AfB_1 molecules but without water was used as a reference state for each line

Although the grid for the energy plots was relatively sparse, it was still evident that the shapes of isoenergetic lines were not parallel to the abscissa axis but were inclined and corresponded partially to isolines of constant basal spacing (Fig. 1). The two water-layer structure of AfB_1-water-smectite complex may thus be the most energetically preferable and stable one. The initial AfB_1 molecules in the complex had the smallest (and preferable) energy of adsorption, but with increasing amounts of interlayer AfB_1, addition of AfB_1 molecules became less preferable (e.g. for Mnt04_Ba, 7.5 mol/kg H_2O, and 0.185 mol/kg AfB_1 it is –23 kcal/mol, but for 0.37 mol/kg AfB_1 adsorbed it is –14 kcal/mol – Fig. 4).

The potential energies of water molecule adsorption, $\Delta U(N)_{H2O}$, on smectites with a constant number of AfB_1 molecules showed that structures with 0.185 mol/kg of AfB_1 had the smallest energies compared to all other AfB_1 contents and also dry structures (blue lines in Fig. 5). With the increase in AfB_1 contents, the addition of water molecules to the structure was energetically less favorable (green, orange, red, and brown lines in Fig. 5).

The initial decrease in energies for 0.185 mol/kg AfB_1 structures was related to expansion of interlayer space and the existence of vacuum easily accessible by H_2O molecules. This led to easier access by water molecules to the interlayer ions. The increase in potential energies of adsorption was caused by relative hydrophobicity of AfB_1 molecules. With increase in water content in the interlayers, the potential energy of H_2O adsorption also increased, which was related mainly to filling of coordinating spheres of cations, around which water molecules were sorbed preferentially (e.g. Fig. 2b).

These molecular simulation results confirmed the assumption that in the interlayer space of smectite, AfB_1 molecules filled the available surface area between those domains covered by the hydrated ions (Deng et al., 2012). Note, however, that the plots in Fig. 4 were received for a certain number of water molecules, which was a value that did not correspond directly to humidity. This was because, depending on the type of interlayer cation for the same humidity, the number of adsorbed water molecules was found to be different (e.g. Laird, 2006).

Influence of Interlayer Cation on the Structure of Aflatoxin-clay Complex

The calculated energy plots of AfB_1, $\Delta U(N)_{AfB1}$, and H_2O molecule adsorption, $\Delta U(N)_{H2O}$, showed substantial differences between divalent (Ba^{2+} and Ca^{2+}) and monovalent (Na^+) cations (Figs. 4b, d, h and 5b, d, h). Both energies were much greater for monovalent ions for various AfB_1 and water contents. For Ca^{2+} and Ba^{2+} the plots were approximately the same.

The values of $\Delta U(N)_{H2O}$ for the Mnt04_Na structure (Fig. 5h) showed less dependence on the absolute water content than structures with divalent ions (Fig. 5b, d). All these observations could be attributed mainly to the differences in hydration enthalpy of the ions: Na^+, –406 kJ/mol; Ca^{2+}, –1579 kJ/mol;

https://doi.org/10.1007/s42860-023-00219-7 Published online by Cambridge University Press

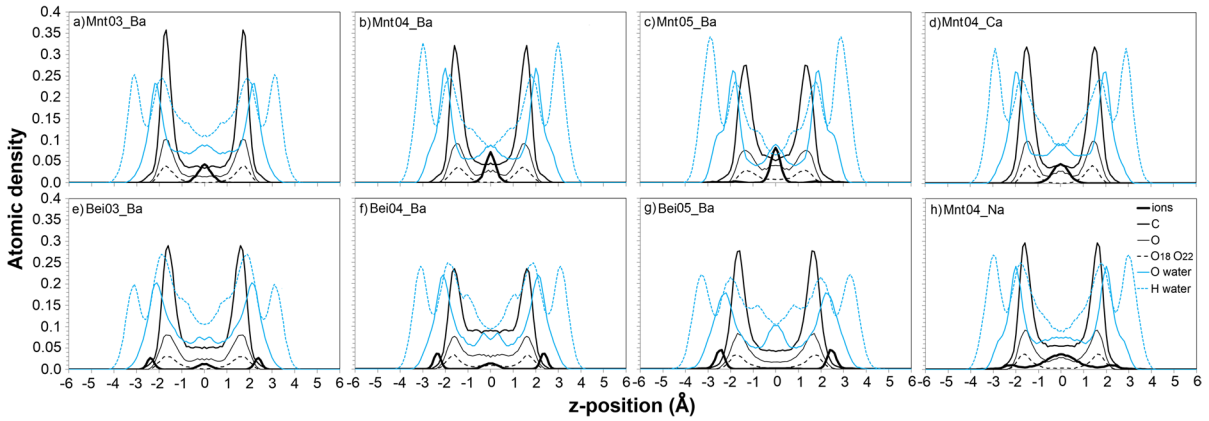

Fig. 6 Distribution of atoms in the interlayer for the structures studied with 0.37 mol/kg of AfB_1 and 7.5 mol/kg of water contents. O18 and O22 are the carbonyl oxygens of AfB_1

and Ba^{2+}, –1309 kJ/mol (Smith, 1977), as H_2O was mainly in the coordination spheres of interlayer cations (Fig. 2b, c).

The differences for $\Delta U(N)_{AfB1}$ (Fig. 4b, d, h) were related rather to available space for AfB_1 adsorption on the surface. The divalent cations form only outer-sphere complexes in the center of Mnt04 interlayers (Fig. 6b, d), while monovalent Na^+ ions tended to form both outer-sphere and inner-sphere complexes at the surface (Fig. 6h). Thereby, Na^+ ions are steric hindrances for hydrophobic AfB_1 molecules (thick black lines in Fig. 6h – some Na^+ ions are close to the surface). For the same number of AfB_1 and H_2O molecules, the maxima of carbon and oxygen atoms of AfB_1 at the surface were slightly greater for divalent ions (thin black lines in Fig. 6b, d, h). In parallel, the plateau in the center of the interlayer for these atoms had greater atomic density for structures with Na^+ ions (for the z-position around zero in Fig. 6b, d, h). The results above are in good agreement with experimental data which shows that smectites with divalent cations are much better adsorbers of AfB_1. According to Deng et al. (2012), this is related to a better size match between AfB_1 molecules and the adsorbing sites on smectite; in the case of divalent cations the hydrophobic smectite surface is more accessible to AfB_1 molecules and this is reflected in Fig. 6b, d, h.

Calculation of RDFs and RCNs for structures corresponding to 0.37 mol AfB_1 and 7.5 mol of water per kg of clay showed that differences in the hydration enthalpies of interlayer ions played an important role in the number of water bridges formed between ions and AfB_1 molecules of the same valency (Fig. 7); the more negative the hydration enthalpy, the more water bridges form between AfB_1 molecule and cations – in the case of Ba^{2+} ions there were clearly more direct ion–dipole interactions than for the Ca^{2+} form (as visible on RCN plots – Fig. 7a). For the Na^+ form, the number of ion–dipole interactions was greater because of the larger number of ions in the interlayer, but the distances of water bridges were less localized (as visible on RDF plots – Fig. 7a). Considering the RDF and RCN for pairs: the ions (Ba, Ca or Na) and oxygens of water (Fig. 7b) showed 8-fold coordination of divalent cations and 4-fold coordination for the monovalent Na^+ cation. This effect is clearly related to the water:ion ratio for the systems studied. Generally, the number of cations that coordinate carbonyl oxygens of AfB_1 via direct ion–dipole interactions (RCN plot: Fig. 7a) was inversely proportional to the number of water molecules surrounding the cations in the first coordination spheres (RCN plot: Fig. 7b).

The potential energy of the addition of AfB_1 to pure water was 9.5 kcal/mol. With an increasing number of water molecules in the interlayers, the potential energy of addition of AfB_1 molecules to the structure had values less than addition of AfB_1 to pure water (~0 kcal/mol; Fig. 4). For a hydration level of 7.5 mol/kg, the energy of addition of AfB_1 molecules to a clay complex could even be <–20 kcal/mol for the first AfB_1 molecules adsorbed (Fig. 4a, b, d).

https://doi.org/10.1007/s42860-023-00219-7 Published online by Cambridge University Press

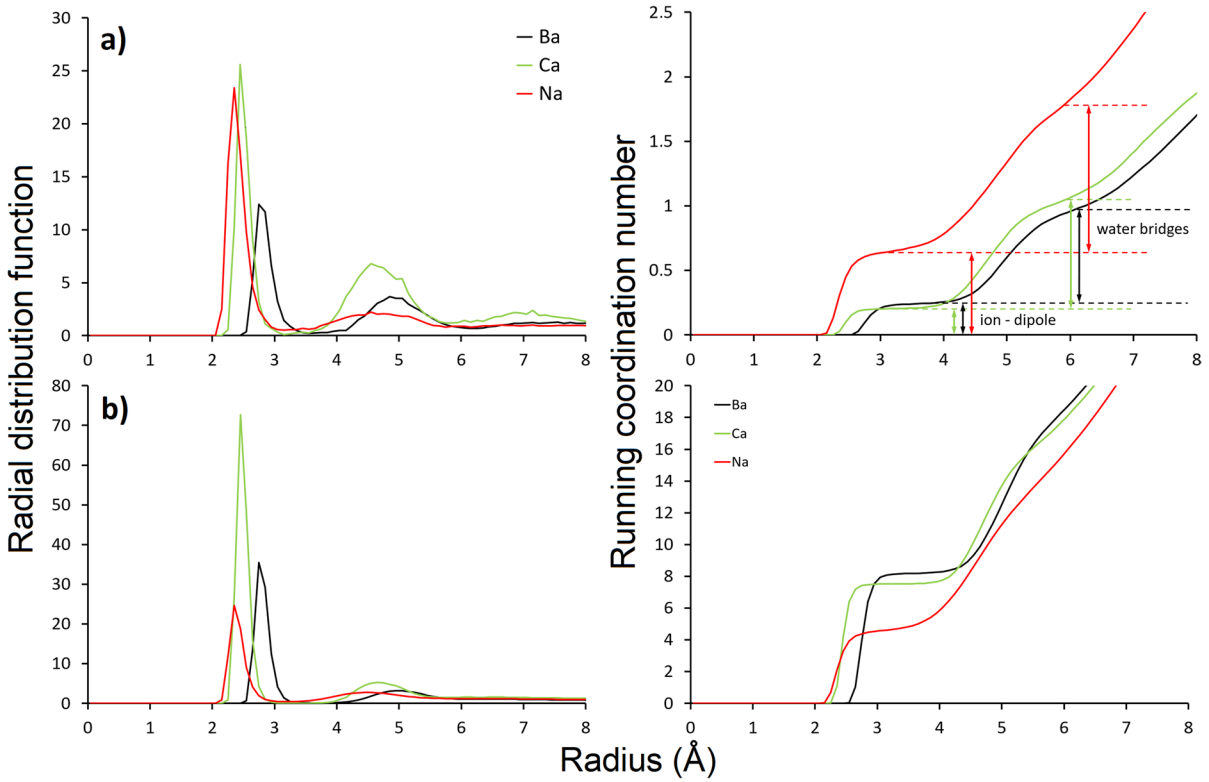

Fig. 7 Radial distribution functions and running coordination numbers for: **a** carbonyl oxygens–interlayer cations; **b** cations–oxygen of water molecules, for montmorillonite with a charge of 0.4 per $O_{10}(OH)_2$ substituted with different ions – 0.37 mol/kg AfB_1 and 7.5 mol/kg of water sorbed

To explain differences in energy of aflatoxin adsorption, the contributions of different energy terms to the total energy of AfB_1 addition were calculated (Eqs. 2 and 3; Table 1). Clearly, the largest differences between smectites were in the electrostatic terms. A less negative term in Na-montmorillonite indicated weaker interactions between the ions, the atoms of the surface and the AfB_1 molecules. These observations are in agreement with experimental results that showed poor AfB_1 adsorption on Na-montmorillonites (Deng et al., 2012; Barrientos-Velazquez et al., 2016b).

In the case of addition of AfB_1 to smectite intercalates, a small deformation of molecular structure (the molecular energy term was 79.4–80.0 kcal/mol, similar for each cation) was observed compared to the addition of AfB_1 to water (molecular energy term: 68.5 kcal/mol; Table 1). The introduction of AfB_1 into smectites led to some deformation of the molecules, therefore, but AfB_1 was retained in the interlayer through electrostatic + van der Waals interactions either with ions or with the surface.

Influence of Layer Charge Density of Montmorillonite on Aflatoxin B_1 Adsorption

Aflatoxin adsorption energy, $\Delta U(N)_{AfB1}$, calculated from Eq. 1 for Ba-montmorillonites having layer charges of 0.3, 0.4, and 0.5 cphuc (Fig. 4a, b, c), showed that layer charge had a large influence on the thermodynamics of the addition of AfB_1 to the structure. For less moist conditions, the energy of adsorption was substantially less for low-charge montmorillonite (Fig. 4a). The smallest energy values were observed when the water content was close to 7.5 mol/kg. With increasing numbers of water molecules in the interlayers, the potential energy of the addition of AfB_1 molecules reached greater values; among Mnt_Ba structures, the highest energies were observed for Mnt05_Ba.

https://doi.org/10.1007/s42860-023-00219-7 Published online by Cambridge University Press

Table 1 Energy contribution (kcal/mol) after addition of AfB_1 molecules to montmorillonites with various cations along with the basal spacing of the complexes

Energy term	AfB_1 in vacuum	AfB_1 to water	AfB_1 to Mnt04_Ba*	AfB_1 to Mnt04_Ca*	AfB_1 to Mnt04_Na*
Molecular (bonds + angles + dihedral + improper)	79.9	68.5	79.4	80.0	79.5
Van der Waals	3.4	–25.4	–26.8	–26.1	–23.9
Electrostatic	–43.2	–33.6	–67.1	–67.1	–59.2
Total potential energy	37.2	9.5	–14.2	–12.0	–1.5
Kinetic energy	30.0	31.9	31.1	31.1	31.1
Basal spacing (Å)			15.88	15.80	15.99

*smectite structure assumes addition of 0.37 mol/kg of AfB1 and having 7.5 mol/kg of water

The calculated energy plots for adsorption of H_2O molecules, $\Delta U(N)_{H2O}$, (Fig. 5a, b, c) showed that with an increase in layer charge, the energy of hydration became more negative. This was due to the first water molecules hydrating around ions being bonded more exothermally (e.g. Rudbeck, 2006). If, in the structure, there were more interlayer ions, then, statistically, more water would bond within the first shells of ions. On the other hand, with increasing numbers of water molecules, clay layers moved further apart. For higher charge-density smectites, clay layers tended to be closer to each other than for low-charge smectites, which could eventually lead to reduction of the amount of intercalated water molecules in experimental studies.

Visualizations of distributions of atoms (Fig. 6a, b, c) showed lower intensity maxima of carbon and oxygen atoms of AfB_1 at the surface for Mnt05_Ba, compared to Mnt03_Ba and Mnt04_Ba. The plateau in the center of the interlayer was, therefore, greatest for high-charge montmorillonite, indicating that AfB_1 molecules were more disordered and farther from the surface for this smectite. The basal spacing was smaller for the high-charge montmorillonite, which indicated squeezing of interlayer molecules (Table 2). Another distinct difference in these complexes was the location of the interlayer cations; they stayed in the middle of the interlayer space in the lower charge-density montmorillonite, and they stayed both in the middle and closer to basal oxygens of montmorillonite with charge density of 0.5 per half unit cell.

Analysis of the potential energy contribution showed differences in the electrostatic term (Table 2). With increase in smectite charge, the attraction between interlayer cations and the clay layer became much stronger and aflatoxin molecules were more squeezed within interlayer spaces, especially for montmorillonite. This resulted in an increase of the electrostatic term and a decrease in the van der Waals term, with increasing montmorillonite layer charge (Table 2). The effect of layer charge on AfB_1 molecules suggested that the interlayer of high-charge smectites was not favored.

The layer charge on a montmorillonite was varied by Barrientos-Velazquez et al. (2016b), who observed that an optimal layer charge was critical for maximum AfB_1 adsorption. Increasing the exchange capacity to >85 cmol/kg decreased significantly the aflatoxin adsorption capacity of montmorillonite. All the results achieved with the modeling, therefore, agreed quite well with those from experiment.

Influence of Location of the Layer Charge on Aflatoxin B_1 Adsorption

The influence of the location of the layer charge on aflatoxin B_1 adsorption was investigated by comparing AfB_1-beidellite with the AfB_1-montmorillonite complexes. Plots of the energy of aflatoxin adsorption on beidellite (Fig. 4e, f, g) showed that adsorption of AfB_1 on smectites with layer charge located in the tetrahedral sheet was much less favorable thermodynamically than if the charge was located in the octahedral sheet. This was because the interlayer ions tended to be located close to the basal surface in beidellites (thick black lines in Fig. 6e, f, g), while they tended to stay in the middle of the interlayers in montmorillonites (thick black lines in Fig. 6a, b, c). If the ions were

https://doi.org/10.1007/s42860-023-00219-7 Published online by Cambridge University Press

Table 2 Energy contribution (kcal/mol) after addition of AfB_1 molecules to smectites with various layer charges along with basal spacing of the complexes

Energy term	AfB_1 to water	AfB_1 to Mnt03_Ba*	AfB_1 to Mnt05_Ba*	AfB_1 to Bei03_Ba*	AfB_1 to Bei04_Ba*	AfB_1 to Bei05_Ba*
Molecular (bonds + angles + dihedral + improper)	68.5	79.2	81.0	78.6	78.9	79.9
Van der Waals	–25.4	–24.6	–27.0	–20.3	–21.6	–23.0
Electrostatic	–33.6	–68.3	–63.5	–63.2	–54.5	–43.2
Total potential energy	9.5	–13.8	–9.4	–4.9	2.8	13.7
Kinetic energy	31.9	31.1	31.1	31.1	31.1	31.1
Basal spacing (Å)		16.28	15.67	16.20	16.07	16.33

*smectite structure assumes addition of 0.37 mol/kg of AfB1 and having 7.5 mol/kg of water

located in the middle of the interlayer space, they had more freedom to adapt to optimal positions between AfB_1 molecules, while if the cations were directly on the clay surface they could expel AfB_1 molecules from the surface and formation of π–π stacking-complexes was more restricted. The distribution of the cations in the interlayer provides an explanation for the experimental AfB_1 adsorption in montmorillonite and beidellite observed by Barrientos-Velazquez et al. (2016b). Greater aflatoxin adsorption by octahedral charged smectites (hectorite and montmorillonite) was observed when compared to tetrahedral charged smectites (beidellite and nontronite).

Ba-montmorillonite with a different location of layer charge in comparison to Ba-beidellite showed generally less negative values of $\Delta U(N)_{H2O}$ and, thus, a smaller gradual increase of $\Delta U(N)_{H2O}$ with increase in the amount of adsorbed water (Figs. 5a, b, c vs. 5e, f, g). This is related to partial hydrophilicity of the beidellite surface in comparison to montmorillonite (Szczerba et al., 2020), which results in smaller values of $\Delta U(N)_{H2O}$ for smaller amounts of water in the structures.

Comparison of energy contributions after addition of AfB_1 molecules to beidellites (Table 2) showed large variations in the electrostatic contribution compared to montmorillonites. In the case of beidellites, the ions were located in the positions close to substitutions in the tetrahedral sheets, and closer to the smectite surface (Fig. 6e, f, g). Ions were less mobile, only partially hydrated in closed shell positions, and, therefore, the electrostatic term was much greater for high-charge beidellites (Table 2). Generally, van der Waals terms decreased with the increase in layer charge, but electrostatic terms increased much more, resulting in a net increase of potential energy for high tetrahedrally charged smectites. These results were confirmed by an experimental test in which the aflatoxin affinity was significantly lower in nontronite, which is a tetrahedrally charged smectite, compared to montmorillonite (Barrientos-Velazquez et al., 2016b).

Conclusions

In addition to verifying the effects of mineralogical properties on aflatoxin–smectite interactions observed experimentally, the molecular simulation offered more insight into the mechanisms that would be difficult to reveal experimentally. Five major conclusions on aflatoxin–smectite interactions were drawn from the molecular simulations:

(1) In all of the AfB_1–smectite complexes studied, substantial amounts of organic molecules tended to be lying flat on the clay surface.
(2) With larger amounts of adsorbed AfB_1 molecules in the structures and/or depending on water content, self-association of two AfB_1 molecules bound by π–π interaction and with each of the molecules lying flat on the clay surface was thermodynamically favorable.
(3) With increasing water content, the interaction of AfB_1 molecules with water tended to remove some of the molecules from the clay surface. Simultaneously, some π–π interactions could break. Locally, three or more AfB2 molecules

https://doi.org/10.1007/s42860-023-00219-7 Published online by Cambridge University Press

could form the π–π stacking complexes in the interlayer under increased water-content conditions. This type of information could not be obtained by experimental methods as, in general, the AfB_1-smectite complexes were characterized under dried conditions when spectroscopic or microscopic methods were employed.

(4) The thermodynamics of AfB_1 adsorption on smectites depended heavily on the water content in the structure, but the adsorbed AfB_1 molecules affected only slightly the thermodynamics of water adsorption. It could, therefore, be concluded that, depending on the humidity, the amounts of AfB_1 adsorbed by smectite can vary.

(5) The potential energy of AfB_1 adsorption on smectites was greater for high-charge smectites and for smectites for which the layer charge originated in the tetrahedral sheet, which reduced the aflatoxin adsorption.

Acknowledgements We are very thankful for the helpful comments by the Editor-in-Chief, the Associate Editor, and by two anonymous reviewers. The authors acknowledge financial support from the United States Department of Agriculture. This work was also supported by the Polish Grid Infrastructure PL-Grid infrastructure.

Code Availability Not applicable

Authors' contributions Marek Szczerba: molecular simulations, analysis of results, writing manuscript, Youjun Deng: revision of data, writing manuscript, Mariola Kowalik: molecular simulations.

Funding United States Department of Agriculture, PLGRID.

Data Availability On request from Marek Szczerba.

Declarations

Conflicts of Interest Not applicable.

References

Awuor, A. O., Yard, E., Daniel, J. H., Martin, C., Bii, C., Romoser, A., Oyugi, E., Elmore, S., Amwayi, S., Vulule, J., Zitomer, N. C., Rybak, M. E., Phillips, T. D., Montgomery, J. M., & Lewis, L. S. (2017). Evaluation of the efficacy, acceptability and palatability of calcium montmorillonite clay used to reduce aflatoxin B1 dietary exposure in a crossover study in Kenya. *Food Additives & Contaminants, Part A, 34*, 93–102.

Barrientos-Velazquez, A. L., & Deng, Y. (2020). Reducing competition of pepsin in aflatoxin adsorption by modifying a smectite with organic nutrients. *Toxins, 12*, 28.

Barrientos-Velazquez, A. L., Arteaga, S., Dixon, J. B., & Deng, Y. (2016a). The effects of pH, pepsin, exchange cation, and vitamins on aflatoxin adsorption on smectite in simulated gastric fluids. *Applied Clay Science, 120*, 17–23.

Barrientos-Velazquez, A. L., Marroquin Cardona, A., Liu, L., Phillips, T., & Deng, Y. (2016b). Influence of layer charge origin and layer charge density of smectites on their aflatoxin adsorption. *Applied Clay Science, 132-133*, 281–289.

Berendsen, H. J. C., Postma, J. P. M., van Gunsteren, W. F., & Hermans, J. (1981). Interaction models for water in relations to protein hydration. In B. Pullman (Ed.), *Intermolecular Forces* (The Jerusalem Symposia on Quantum Chemistry and Biochemistry) (Vol. 14, pp. 331–342). Springer.

Colvin, B. M., Sangster, L. T., Haydon, K. D., Beaver, R. W., & Wilson, D. M. (1989). Effect of a high affinity aluminosilicate sorbent on prevention of aflatoxicosis in growing pigs. *Veterinary and Human Toxicology, 31*, 46–48.

Cygan, R. T., Liang, J. J., & Kalinichev, A. G. (2004). Molecular models of hydroxide, oxyhydroxide, and clay phases and the development of a general force field. *Journal of Physical Chemistry B, 108*, 1255–1266.

Deng, Y., & Szczerba, M. (2011). Computational evaluation of bonding between aflatoxin B1 and smectite. *Applied Clay Science, 54*, 26–33.

Deng, Y., Barrientos-Velazquez, A. L., Billes, F., & Dixon, J. B. (2010). Bonding mechanisms between aflatoxin B1 and smectite. *Applied Clay Science, 50*(1), 92–98.

Deng, Y., Liu, L., Barrientos-Velazquez, A. L., & Dixon, J. B. (2012). The determinative role of the exchange cation and layer-charge density of smectite on Aflatoxin adsorption. *Clays and Clay Minerals, 60*, 374–386.

Jaynes, W., Zartman, R., & Hudnall, W. (2007). Aflatoxin B1 adsorption by clays from water and corn meal. *Applied Clay Science, 36*(1-3), 197–205.

Kannewischer, I., Tenorio, A. M. G., White, G. N., & Dixon, J. B. (2006). Smectite clays as adsorbents of aflatoxin B1: Initial steps. *Clay Science, 12*(Supplement 2), 199–204.

Khan, A., Akhtar, M. S., Akbar, S., Khan, K. S., Iqbal, M., Barrientos-Velazquez, A. L., & Deng, Y. (2022). Effects of Metal-Polycation Pillaring and Exchangeable Cations on Aflatoxin Adsorption by Smectite. *Clays and Clay Minerals, 70*, 155–164.

Kubena, L. F., Harvey, R. B., Huff, W. E., & Corrier, D. E. (1990). Efficacy of a hydrated sodium calcium aluminosilicate to reduce the toxicity of aflatoxin and T-2 toxin. *Poultry Science, 69*, 1078–1086.

Laird, D. A. (2006). Influence of layer charge on swelling of smectites. *Applied Clay Science, 34*, 74–87.

Magnoli, A. P., Cabaglieri, L. R., Magnoli, C. E., Monge, J. C., Miazzo, R. D., Peralta, M. F., Salvano, M. A., Rosa, C. A. R., Dalcero, A. M., & Chiacchiera, S. M. (2008). Bentonite performance on broiler chickens fed with diets

containing natural levels of aflatoxin B1. *Revista Brasileira De Medicina Veterinaria, 30*, 55–60.

Maki, C. R., Thomas, A. D., Elmore, S. E., Romoser, A. A., Harvey, R. B., Ramirez-Ramirez, H. A., & Phillips, T. D. (2016). Effects of calcium montmorillonite clay and aflatoxin exposure on dry matter intake, milk production, and milk composition. *Journal of Dairy Science, 99*, 1039–1046.

Masimango, N., Remacle, J., & Ramaut, J. (1979). Elimination of aflatoxin B1 from contaminated media by swollen clays. *Annales de la Nutrition et de l'Alimentation, 33*, 137–147.

Mitchell, N. J., Xue, K. S., Lin, S., Marroquin-Cardona, A., Brown, K. A., Elmore, S. E., Tang, L., Romoser, A., Gelderblom, W. C., Wang, J. S., & Phillips, T. D. (2014). Calcium montmorillonite clay reduces AFB1 and FB1 biomarkers in rats exposed to single and co-exposures of aflatoxin and fumonisin. *Journal of Applied Toxicology, 34*, 795–804.

Phillips, T. D., Kubena, L. F., Harvey, R. B., Taylor, D. R., & Heidelbaugh, N. D. (1988). Hydrated sodium calcium aluminosilicate: A high affinity sorbent for aflatoxin. *Poultry Science, 67*, 243–247.

Plimpton, S. (1995). Fast parallel algorithms for short-range molecular dynamics. *Journal of Computational Physics, 117*, 1–19.

Pollock, B. H., Elmore, S., Romoser, A., Tang, L., Kang, M. S., Xue, K., Rodriguez, M., Dierschke, N. A., Hayes, H. G., Hansen, H. A., Guerra, F., Wang, J. S., & Phillips, T. (2016). Intervention trial with calcium montmorillonite clay in a south Texas population exposed to aflatoxin. *Food Additives & Contaminants, Part A, 33*, 1346–1354.

Rudbeck, M. (2006). Potassium(I) in water from Theoretical Calculations. Diploma thesis, Department of Mathematics, Uppsala University, Uppsala, Sweden, pp. 51.

Smith, D. W. (1977). Ionic hydration enthalpies. *Journal of Chemical Education, 54*, 540–541.

Szczerba, M., Kalinichev, A. G., & Kowalik, M. (2020). Intrinsic hydrophobicity of smectite basal surfaces quantitatively probed by molecular dynamics simulations. *Applied Clay Science, 188*, 105497.

Wang, J., Wolf, R. M., Caldwell, J. W., Kollman, P. A., & Case, D. A. (2004). Development and testing of a general amber force field. *Journal of Computational Chemistry, 25*, 1157–1174.

Wang, W., Tian, G., Zong, L., Zhou, Y., Kang, Y., Wang, Q., & Wang, A. (2017). From illite/smectite clay to mesoporous silicate adsorbent for efficient removal of chlortetracycline from water. *Journal of Environmental Sciences (China), 51*, 31–43.

https://doi.org/10.1007/s42860-023-00219-7 Published online by Cambridge University Press